

OR2-4

TEXUS ロケットによる微小重力環境での正デカン液滴列
に沿った冷炎燃え広がり挙動Cool Flame Spread Behavior along *n*-Decane Droplet
Array under Microgravity by a TEXUS Rocket

齊藤允教¹, 菅沼祐介¹, 家村和輝¹, 高畑優星¹, Martínez Figueira Noelia², Meyer Florian²,
Eigenbrod Christian², 野村浩司¹, 田辺光昭¹
Masanori SAITO¹, Yusuke SUGANUMA¹, Kazuki IEMURA¹, Yusei TAKAHATA¹,
Noelia MARTÍNEZ FIGUEIRA², Florian MEYER², Christian EIGENBROD²,
Hiroshi NOMURA¹ and Mitsuaki TANABE¹

¹ 日本大学, Nihon University,

² ZARM, Bremen University

1. Introduction

We conducted the microgravity experiment by the TEXUS#60 sounding rocket to elucidate the cool flame dynamics. Cool flame appears as a result of the low temperature oxidization mechanism preceding the hot flame from the normal alkane that is the major component of jet fuel including Sustainable Aviation Fuel (SAF) and plays a key role in a whole ignition process. In the case of the low temperature reaction, the balance of the dissipation of heat/species (physical characteristics) and the reaction (chemical characteristics) determines the ignition. Therefore, to fundamentally model the cool flame combustion, the experiment of the microgravity environment that achieve the simple system without natural convection is necessary. The Japan and Germany science group have been proceeding the “Phoenix-2” project¹⁻³. The scope of the project is to understand the cool flame behavior such as spontaneous ignition and cool flame spreading near the ignition limit which is useful to clarify the influence of the dissipation sensitively because the reaction speed is very slow. In this paper, the cool flame spread behavior is reported. Mikami et al., studied the cool flame can spreads among the multi-fuel droplets even though they are apart exceeding the distance of hot flame spread limit⁴. Saito et al. conducted the cool flame spread experiment by the forced ignition with the ambient temperature of 293 K to 298 K which is the lower condition of the cool flame spontaneous ignition limit⁵. Because cool flame affects the hot flame behavior, the spread behavior such as the speed, spread limit, etc. need to be elucidated. In the Phoenix-2 experiment, we expect the cool flame propagation in two experimental conditions; one is a dense array consisting of nine droplets in 8 mm spacing, the other is a sparse array consisting of five droplets in 16 mm spacing. Mikami’s and Saito’s experiment, the cool flame may spread by the species and the heat transfer to the neighbor droplet because their ambient temperatures are much lower than the spontaneous ignition limit. On the other hand, our experimental condition is near the spontaneous ignition limit, the cool flame spread may be driven by not only the heat and the species transportation but also chemical reaction. In this

report, we evaluate the flame spread behavior focusing on the flame spread speed.

2. Experimental Configuration

The Droplet array Combustion Unit 2 (DCU2) is integrated on the payload of the TEXUS#60. For the detail system configuration, please refer to the past paper². The emission from the cool flame was captured by an intensified high-speed camera (Lambert, HICAM 500ST) through a lens (SIGMA, 135 mm, F1.8) and a band pass filter (CWL: 400 nm, FWHM: 50 nm). The droplet diameters are measured by two CCD cameras (Image source, DMK33UJ003) with backlit. The DCU2 has two combustion furnaces whose ambient temperatures are 570 K (unit 1) and 590 K (unit 2). Two cool flame images from both furnaces are able to be captured by a prism mirror. Since the unit 2 of 590 K did not work, only the result of 570 K is reported in this paper. The spatial resolutions of the high-speed camera and the CCD camera of the unit 1 are 14.9 pix/mm and 49.5 pix/mm respectively. The detail configuration is shown in the left of Fig. 1. The droplets and thermocouple locations are shown in the right of Fig. 1. For the cool flame spread, we employed two droplet arrangement patterns; one is the nine droplets (dense array pattern) with inter-droplet spacing S of 8 mm, and five droplets (sparse array pattern) with inter-droplet spacing of 16 mm. The furnace has five K-type thermocouples whose diameters of 1.0 mm (TC1 thru TC5).

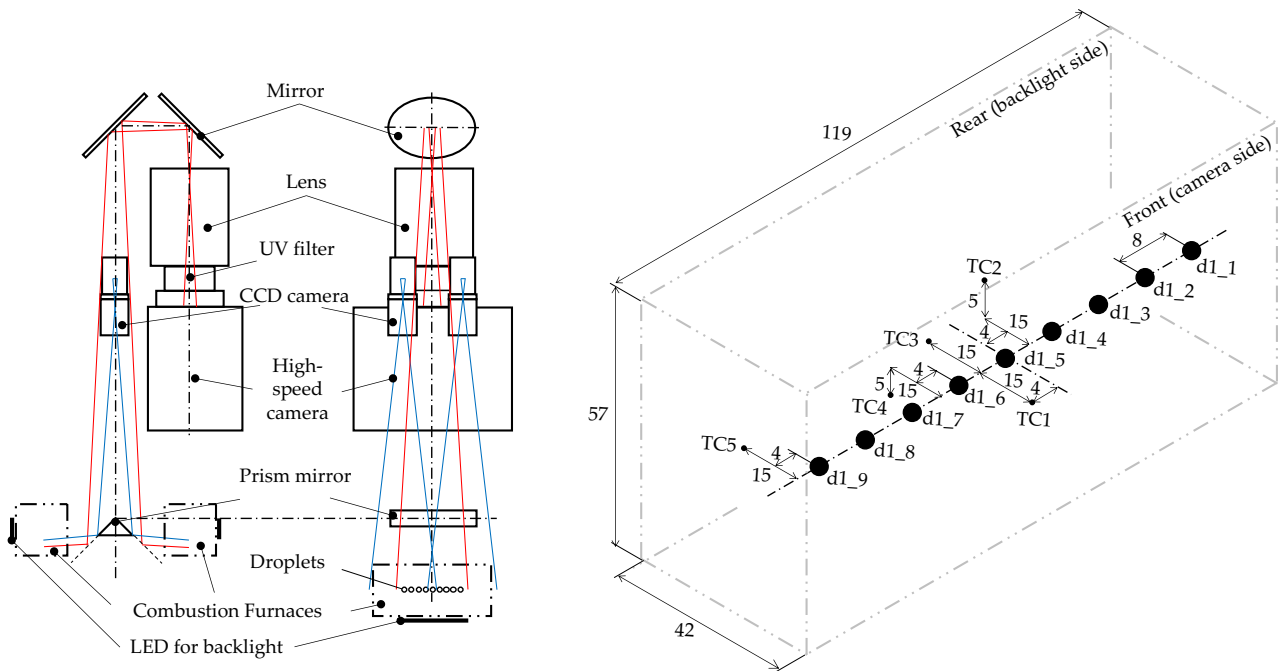


Figure 1. Schematic of the component layout (left) / the position of the fuel droplet (d1_1 thru d1_9) and the tips of thermocouples (TC1 thru TC5) with inner dimension of the combustion furnace (right).

3. Results and Discussion

Figure 2 shows the measured temperature distribution in the combustion furnace for $S = 8$ mm condition (left) and $S = 16$ mm condition (right) respectively. The time zero corresponds to the droplet array stop time at the combustion position. The target temperature was 570 K, however, the actual initial ambient temperature was approximate 565 K. After settling the droplets at the combustion position, temperatures are slightly decrease by fuel evaporation, then it turns to increase after about 7 s past due to ignition. The temperature rises were approximate 10 K.

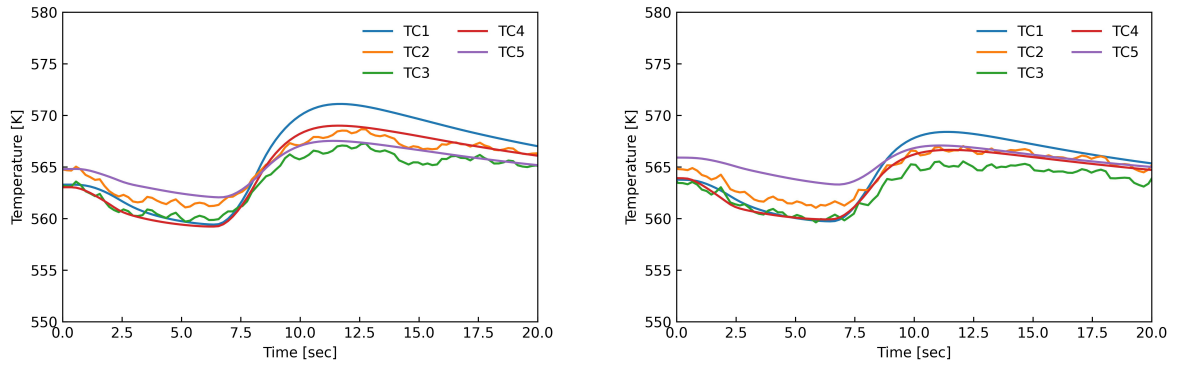


Figure 2. Measured temperature in the furnace using TC1 thru TC5 of $S = 8$ mm (left) and 16 mm (right) conditions.

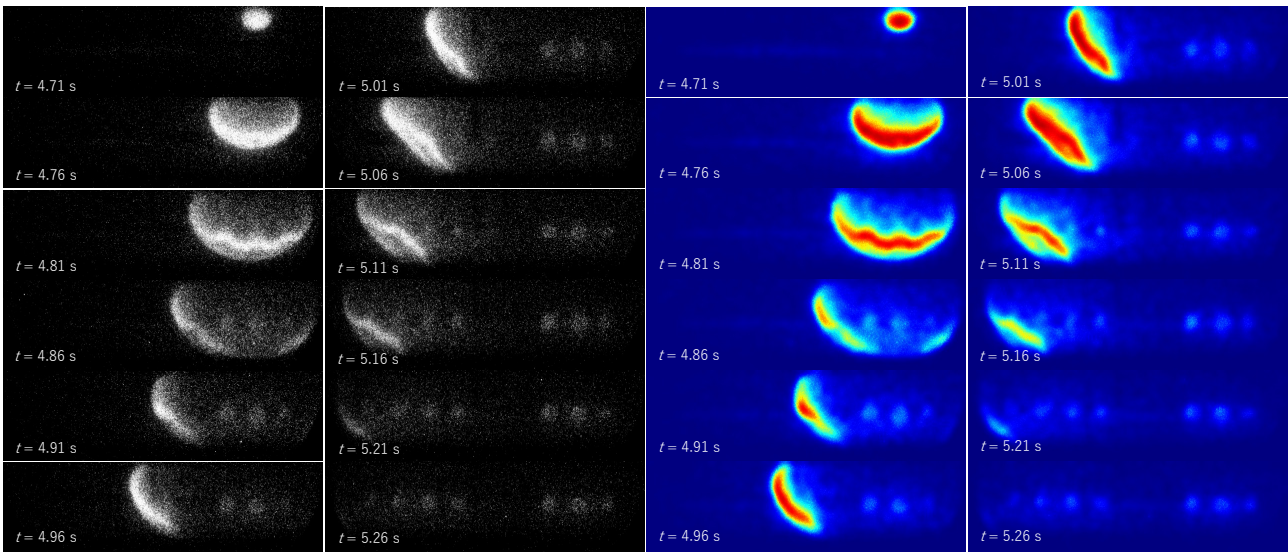


Figure 3. Raw (left) and processed images (right) of the high-speed intensified images for cool flame spread of $S = 8$ mm condition.

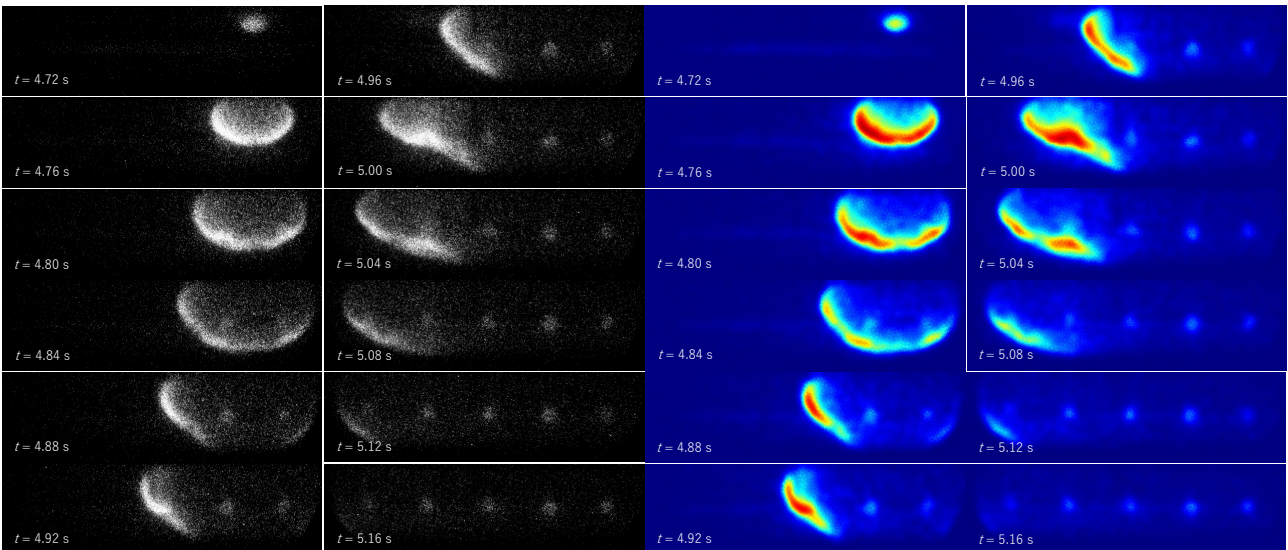


Figure 4. Raw (left) and processed images (right) of the high-speed intensified images for cool flame spread of $S = 16$ mm condition.

Figures 3 and 4 show the high-speed sequential images of cool flame spread of $S = 8$ and 16 mm respectively. The left two columns are the raw images. The backgrounds of these images were subtracted by averaged images over 100 frames without the cool flame emission, and then were applied by the Bilateral filter whose kernel size of 41×41 pixels, the smoothing parameter for the pixel distance of 150, and for the luminosity difference of 150 to reduce the noise with keeping the leading edge structure of the cool flame. In the case of $S = 8$ mm condition, the generation for droplet d1_4 was not successful.

The cool flames appeared after 4.71 s for $S = 8$ mm and 4.72 s for $S = 16$ mm respectively. For both cases, the flames appeared near the top wall of the furnace where the axial position corresponds with the d1_2 droplet. If the initial ambient temperature in the furnace is homogeneous, the cool flame is expected to occur from both ends of the array from the past numerical simulations⁶. Therefore, the temperature inhomogeneity may have existed in the furnace. During the spread, the leading edge traveled along slightly apart from the droplet. So, it is thought that the fuel mixture well established around the droplet and the flame spread along this mixture layer. After the spread, all droplets established the steady cool flames in $S = 16$ mm, whereas d1_4 which was not successful, and d1_5 did not establish them in $S = 8$ mm.

To evaluate the spread speed, the leading edges were tracked. The filtered images were converted into the binary images by Otsu's method⁷. To avoid the tracking of individual outlier pixels, the most left 255 value pixel whose right four pixels are also 255 value is defined as the leading edge as shown in Fig. 5.

Figure 6 shows the cool flame spread speed calculated by the tracking the leading edge in two ways; one is the lateral tracking method which the speed is calculated by the only axial coordination, and the point tracking method by both axial and vertical coordination. Comparing the two results, there are few differences, so the spread speed is discussed by the lateral track result.

For both cases, the spread speeds changed following the same trend. The first stage just after the spontaneous ignition, spread speeds decreased from approximate 250 mm/s to 100 mm/s within the first second after ignition. After the steady stage after 1-2 s, the speeds turned to increase. The speed of $S = 16$ mm reached around 600 mm/s. This acceleration stage may be driven by the sequential spontaneous ignition along the high reactive mixture. Because the cool flames of $S = 8$ mm and 16 mm finish to spread by $t = 5.26$ s and 5.16 s respectively as seen in Fig. 3 and Fig. 4, the large deviation around $t = 5.2$ s caused by the background noise.

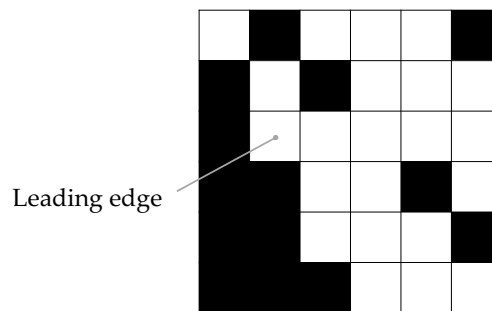


Figure 5. Definition of the leading edge.

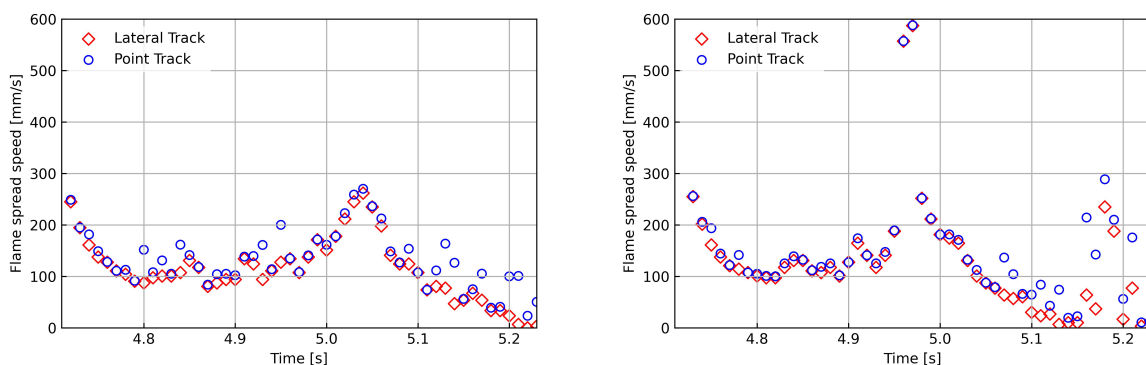


Figure 6. Cool flame spread speed for $S = 8$ mm condition (left) and $S = 16$ mm condition (right).

4. Conclusions

The microgravity experiment “Phoenix-2” using the TEXUS#60 sounding rocket to elucidate the cool flame dynamics near the spontaneous ignition limit succeeded. The cool flame spread behavior focusing on its spread speed was analyzed and the followings are found.

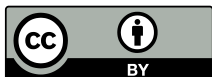
1. Both $S = 8$ mm and 16 mm cases, the cool flame occurred almost the same position after 4.7 s past from the droplet inserted and settling the combustion position.
2. The cool flame spread speed firstly decreased to around 100 mm/s, then turned to increase, and finally reached around 600 mm/s in $S = 16$ mm condition. It is thought that the acceleration may be driven by the sequential spontaneous ignition.

Acknowledgements

This study was supported by ISAS-JAXA as *The Front-Loading Project* and *Small-Scale Project*, by JSPS KAKENHI Grant Number JP19K04843 and JP21K14347, and by Nihon University President Grant Initiative. The DCU2 development and its integration for the TEXUS rocket were supported by IHI Inspection & Instrument Co., Ltd. and Airbus Defense and Space. On the German side, this experiment was funded by the German Space Agency at DLR.

References

- 1) M. Tanabe, M. Saito, Y. Suganuma, M. Mikami, M. Kikuchi, Y. Inatomi, O. Moriue and H. Nomura: Scope of PHOENIX-2 Sounding Rocket Experiment, “Cool Flame Dynamics in Multi-droplet Ignition”, *Int. J. Sci. Appl.* **37** (4) (2020) 370401-1, DOI: [10.15011/jasma.37.4.370401](https://doi.org/10.15011/jasma.37.4.370401).
- 2) Y. Suganuma, M. Saito, Y. Goto, S. Yamamoto, M. Nokura, M. Mikami, M. Kikuchi, Y. Inatomi, O. Moriue, H. Nomura and M. Tanabe: Hardware Development for Cool Flame Combustion Experiment of Fuel Droplets using Sounding Rocket, *Int. J. Sci. Appl.* **37** (4) (2020) 370403-1, DOI: [10.15011/jasma.37.4.370403](https://doi.org/10.15011/jasma.37.4.370403).
- 3) M. Saito, Y. Ohno and M. Tanabe: Numerical Study on the Cool Flame Dynamics of *n*-Decane Fuel Droplets by 2D Simulation with Gas-Liquid Equilibrium, *Int. J. Sci. Appl.* **37** (4) (2020) 370402-1, DOI: [10.15011/jasma.37.4.370402](https://doi.org/10.15011/jasma.37.4.370402).
- 4) M. Mikami, K. Matsumoto, Y. Chikami, M. Kikuchi and D. L. Dietrich: Appearance of Cool Flame in Flame Spread over Fuel Droplets in Microgravity, *Proc. Combust. Inst.* **39** (2) (2023) 2449, DOI: [10.1016/j.proci.2022.07.053](https://doi.org/10.1016/j.proci.2022.07.053).
- 5) I. Saito, S. Shinkai, H. Nomura and Y. Suganuma: Development of Forced Cool-Flame Ignition and Detection Device for a Fuel Droplet, *Int. J. Sci. Appl.* **39** (3) (2022) 390303-1, DOI: [10.15011/jasma.39.390303](https://doi.org/10.15011/jasma.39.390303).
- 6) M. Saito, Y. Ohno, H. Kato, Y. Suganuma, M. Mikami, M. Kikuchi, Y. Inatomi, T. Ishikawa, O. Moriue, H. Nomura and M. Tanabe: Spontaneous Ignition Behavior of *n*-Decane Fuel Droplet Array near Ignition Limit, *Int. J. Sci. Appl.* **36** (2) (2019) 360205-1, DOI: [10.15011/jasma.36.2.360205](https://doi.org/10.15011/jasma.36.2.360205).
- 7) N. Otsu: A Threshold Selection Method from Gray-Level Histograms, *IEEE Transactions on Systems, Man, and Cybernetics* **9** (1) (1979) 62, DOI: [10.1109/TSMC.1979.4310076](https://doi.org/10.1109/TSMC.1979.4310076).



© 2024 by the authors. Submitted for possible open access publication under the terms and conditions of the Creative Commons Attribution (CC BY) license (<http://creativecommons.org/licenses/by/4.0/>).